

*Regular Article***General anesthetic binding mode via hydration with weak affinity and molecular discrimination: General anesthetic dissolution in interfacial water of the common binding site of GABA<sub>A</sub> receptor**

Tomoyoshi Seto

*Department of Anesthesiology, School of Medicine, Shiga University of Medical Science, Otsu, Shiga 520-2192, Japan*

Received July 4, 2022; Accepted January 23, 2023;

Released online in J-STAGE as advance publication January 25, 2023

Edited by Motonori Ota

The GABA<sub>A</sub> receptor (GABA<sub>A</sub>R) is a target channel for the loss of awareness of general anesthesia. General anesthetic (GA) spans a wide range of chemical structures, such as monatomic molecules, barbital acids, phenols, ethers, and alkanes. GA has a weak binding affinity, and the affinity has a characteristic that correlates with the solubility in olive oil rather than the molecular shape. The GA binding site of GABA<sub>A</sub>R is common to GAs and exists in the transmembrane domain of the GABA<sub>A</sub>R intersubunit. In this study, the mechanism of GA binding, which allows binding of various GAs with intersubunit selectivity, was elucidated from the hydration analysis of the binding site. Regardless of the diverse GA chemical structures, a strong correlation was observed between the binding free energy and total dehydration number of the binding process. The GA binding free energy was more involved in the binding dehydration and showed molecular recognition that allowed for the binding of various GA structures via binding site hydration. We regarded the GA substitution for the interfacial water molecule of the binding site as a dissolution into the interfacial hydration layer. The elucidation of the GA binding mechanism mediated by hydration at the GABA<sub>A</sub>R common binding site provides a rationale for the combined use of anesthetics in medical practice and its combination adjustments via drug interactions.

**Key words:** GABA<sub>A</sub> receptor, general anesthetics, molecular recognition, protein hydration, dissolution**◀ Significance ▶**

GABA<sub>A</sub> receptor is a target channel of general anesthesia. We found a weak general anesthetic (GA) binding mode via hydration and elucidated the mechanism that allows binding of various structures of GA to GABA<sub>A</sub> receptor. The binding energy was involved in the dehydration, allowing for the diversity of GA structures binding to the receptor. We can regard GA substitution for the interfacial water molecule of the binding site as a dissolution into the hydration layer. This study promotes understanding of molecular recognition in GA binding site of GABA<sub>A</sub> receptor and provides basis for clinical anesthesia.

**Introduction**

The elements of general anesthesia include loss of consciousness, analgesia, and immobilization, which can be harnessed based on clinical needs [1]. In practice, different anesthetics are used in combination to achieve clinical design. Recently, it has become clear that postoperative delirium due to general anesthesia affects perioperative life prognosis [2], and there is a concern that general anesthesia may affect the progression of mild cognitive impairment [3]. Currently, the quality of loss of awareness is an issue in anesthesia practice [4].

The principal target for the loss of awareness of general anesthesia is the GABA<sub>A</sub> receptor (GABA<sub>A</sub>R). General anesthetics (GAs) with diverse structures (Figure 1) bind to GABA<sub>A</sub>R channels, resulting in Cl<sup>-</sup> current potentiation [5].

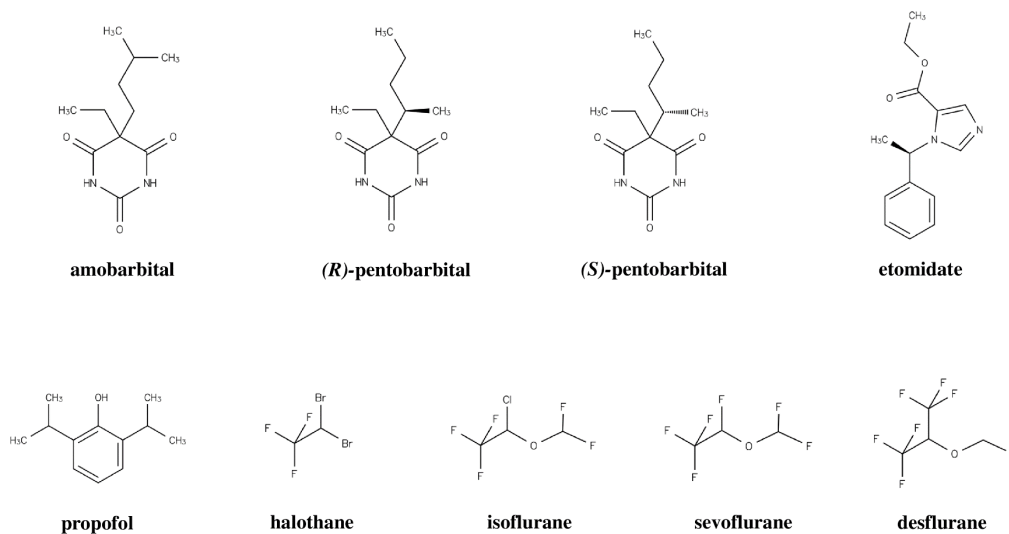


**Figure 1** Structure of general anesthetics

The GABA<sub>A</sub>R is distributed in the inhibitory neurons of the prefrontal cortex, wherein potentiation causes prefrontal cortex suppression. Based on these findings, GABA<sub>A</sub>R is a major molecular target for the loss of awareness caused by general anesthesia [6]. The structure of GABA<sub>A</sub>R consists of five subunits assembled to form a Cl<sup>-</sup> channel. The central nervous system neurons are mainly composed of subunits of the 2 $\alpha_1$ 2 $\beta_3$  $\gamma_2$  composition (Figure 2A, 2B) [7]. The atomic coordinates of the three-dimensional structure of  $\alpha_1\beta_3\gamma_2$  GABA<sub>A</sub>R [Protein Data Bank (PDB) ID: [6i53](#)] have been clarified [8], enabling discussions based on the molecular structure.

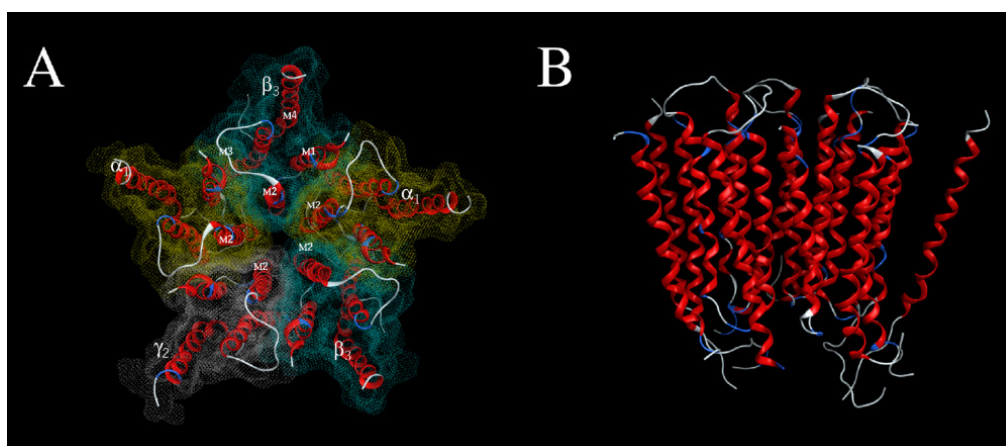


**Figure 2** Secondary structure of transmembrane domain (TMD) of  $\alpha_1\beta_3\gamma_2$  GABA<sub>A</sub> receptor from Protein Data Bank 6i53. **A:** Extracellular view. The GABA<sub>A</sub> receptor comprises a pentamer of subunits. Meshwork represents molecular surface of each subunit. Each subunit consisted of four transmembrane helical bundles (M1, M2, M3, and M4). Five M2 helices of the pentamer consist of channel conduit of Cl<sup>-</sup>. **B:** Side view of TMD.

As for the GA binding site, the amino acid residue in the transmembrane domain (TMD) of the intersubunit was identified by photolabeling and the intersubunit was found to be the common binding site of GA [9]. Sevoflurane has been reported to bind to the  $\alpha_1/\beta_3$ ,  $\beta_3/\alpha_1$  and  $\alpha_1/\gamma_2$  intersubunits of  $\alpha_1\beta_3\gamma_2$  GABA<sub>A</sub>R; with a different binding selectivity compared to isoflurane [10]. In addition, the  $\alpha_1/\gamma_2$  intersubunit is considered an orphan site to which intravenous GA does not bind [11]. These common binding sites allow for the binding of diverse structures of GAs (weak structural selectivity) (Figure 1) while retaining the properties of the intersubunits, such as intersubunit binding selectivity [12].

In general, drugs bind selectively and show high specificity for their binding sites. However, GAs (Figure 1) have unique characteristics: (1) they have a weak binding affinity [13]; (2) the binding site affinity correlates with the solubility in olive oil rather than the molecular shape (Mayer-Overton rule) [14]; (3) the steric discrimination of optical anesthetics is weak (i.e., molecular discrimination of the pentobarbital enantiomer is weak [15]); (4) molecules larger than a specific size have no anesthetic effect (cut-off phenomenon) [16]; and (5) the anesthetic action has the characteristic of pressure antagonism [17,18]. These characteristics not only elucidate the pharmacological action of GAs (i.e., enable the study of the mechanism of anesthesia), but also provide a theoretical background for the modern use of anesthetics, their combinations, side effect control, and drug interaction control, and represent an avenue for solving current topics in the field of clinical anesthesia. A molecular recognition mechanism exists at the GA-binding site, which allows structural diversity. Thus, the study of the GA binding mode of GABA<sub>A</sub>R sites will help elucidate the mechanism of GA binding, which has weak molecular discrimination and allows for the binding of various chemical structures.

The purpose of this study was to identify the GA binding site of GABA<sub>A</sub>R and investigate the binding modes (i.e., position, orientation, and conformation) to identify the mechanism that allows diverse GA binding and intersubunit selectivity. The GA binding site, binding mode, and binding free energy were determined by molecular docking. Docking simulation can predict the crystal structure of the ligand-receptor complex at a low computational cost by incorporating ligand flexibility and partially considering the induced fit of the receptor. Even without known structures, we can predict a ligand-receptor complex structure and estimate the ligand-receptor interactions and binding energies from the predicted structure. The accuracy of structure prediction is highly dependent on the ligand conformer generation algorithm, fitting search algorithm, electrical charges, force fields, etc. We adopted the ASEDock [19] program for the binding mode predictions.

To identify the origin of GA binding affinity to  $\alpha_1\beta_3\gamma_2$  GABA<sub>A</sub>R, GAs with diverse chemical structures, such as amobarbital, (*R*)-pentobarbital, (*S*)-pentobarbital, etomidate, propofol, halothane, isoflurane, sevoflurane, and desflurane, were used (Figure 1). In general, GABA<sub>A</sub>R have multiple binding sites that are not involved in GA action. ASEDock searches for GA binding sites and outputs the binding sites in docking score order. In this study, we investigated the GA binding site involved in GA action (which causes functional modifications) and clarified the characteristics of the GA binding site. Photolabeling GAs with GABA<sub>A</sub>R potentiation, AziSEVO, azietomidate, and (*R*)-mTFD-MPAB, were used to identify pharmacological GA binding sites. GA binding sites having the action were revealed to exist in the intersubunit of the receptor [9,10]. We selected intersubunit binding sites from ASEDock output and investigated the intersubunit binding site of GAs in this study.

The binding affinity of the monatomic molecular anesthetics xenon, krypton, and argon for human serum albumin is mainly due to the hydration effect (hydration energy), and the binding mode does not depend on the shape of the molecule [20]. We investigated changes in the distribution of hydration water molecules before and after GA binding to evaluate their involvement in the binding of hydration energy. The oxygen atom density of the GA binding site (within 20 Å of the GA molecule) was evaluated using the 3D-RISM (reference interaction site model) method [21,22]. From the obtained oxygen atom density of the GA binding sites, the water molecule distribution of the hydration was visualized using the water-mapping method [23]. Hydration analysis was performed using dimer models of subunits to avoid high computational costs. The  $\beta_3/\alpha_1$  dimer model was obtained by extracting the TMD regions of  $\beta_3$  and  $\alpha_1$  subunits (937 residues) of the receptor. To further reduce the amount of calculation, 3D-RISM was limited to 20 Å from the general anesthetic binding. The hybrid method proposed by Hikiri et al. [24] can accurately obtain the hydration energy, and its accuracy has been verified by experimental results. The hybrid method was not employed because the program for the morphometric approach was not open. A strong correlation was found between the GA binding free energy ( $\Delta G_{\text{bind}}$ ) and the dehydration number of the binding process. We found that the binding free energy of the intersubunit did not depend on the shape of the GA molecule. Binding site hydration contributed more than the shape fit, indicating weak molecular discrimination that allows for the binding of various GA structures via hydration. GA binding can be understood as a dissolution process in the intersubunit that replaces the interfacial water with the GA molecule.

## Materials and Methods

### GABA<sub>A</sub>R Structure Preparations

The three-dimensional (3D) structure of GABA<sub>A</sub>R [PDB ID: [6i53](#)] [8] (3.2 Å resolution) was obtained from the Protein Data Bank (PDB). Megabody38 and oligosaccharide molecules included in 6i53 were removed for the docking analysis. The missing hydrogen atoms in the 6i53 structure were also amended. To avoid overlapping of the added hydrogens with heavy atoms and other atoms, the hydrogen positions were optimized by energy minimization. The protonation of 6i53 at pH 7 was conducted using the Molecular Operating Environment (MOE) Protonate 3D program [25]. The complete

GABA<sub>A</sub>R structure at pH 7 (6i53 model), including hydrogen atoms, was used to examine the flexible docking of the GAs.

To evaluate the hydration of TMD in the 6i53 model, a TMD (M1-M2-M3) model was prepared by removing the extracellular domain (ECD), M4 helices, and lipids from the 6i53 model. The TMD model consists of A–E chains corresponding to the pentamer subunit. A-chain ( $\alpha_1$ ) TMD contains amino acid residue 224-318, B-chain ( $\beta_3$ ) contains residue 219-308, C-chain ( $\gamma_2$ ) residue 224-323, D-chain ( $\alpha_1$ ) contains residue 224-313, and E-chain ( $\beta_3$ ) residue 219-308, respectively. For the analysis of binding site hydration,  $\alpha_1/\beta_3$ ,  $\beta_3/\alpha_1$ ,  $\gamma_2/\beta_3$ , and  $\alpha_1/\gamma_2$  intersubunit dimer models were prepared by removing ECD and lipids from the 6i53 model.

### General Anesthetics

To investigate the GA binding site of  $\alpha_1\beta_3\gamma_2$  GABA<sub>A</sub>R, amobarbital: 5-ethyl-5-(3-methylbutyl)-1,3-diazinane-2,4,6-trione, (*R*)-pentobarbital: 5-ethyl-5-[(2*R*)-pentan-2-yl]-1,3-diazinane-2,4,6-trione, (*S*)-pentobarbital: (5-ethyl-5-[(2*S*)-pentan-2-yl]-1,3-diazinane-2,4,6-trione, etomidate: ethyl 3-[(1*R*)-1-phenylethyl]imidazole-4-carboxylate, propofol: 2,6-di(propan-2-yl)phenol, halothane: 2-bromo-2-chloro-1,1,1-trifluoroethane, isoflurane: 2-chloro-2-(difluoromethoxy)-1,1,1-trifluoroethane, sevoflurane: 1,1,1,3,3,3-hexafluoro-2-(fluoromethoxy)propane, and desflurane: 2-(difluoromethoxy)-1,1,1,2-tetrafluoroethane were adopted. The chemical structures of GAs are shown in Figure 1.

### Docking Simulation and Binding Free Energy $\Delta G_{\text{bind}}$ Estimation

MOE (Chemical Computing Group, Inc., Canada) was used to perform three-dimensional presentation, structural preparation, docking program execution, and interaction analysis [26]. The ASEDock program on the MOE platform (MOLSIS Inc., Japan) was used for docking with default parameters and conservation of chirality [19]. ASEDock treats ligands as flexible molecules while maintaining their chirality. The 6i53 backbone atoms were tethered, whereas the side chain remained flexible for docking. We adopted the Amber10: EHT force field to set the partial charge and force field parameters [27,28]. The total binding energy was calculated by molecular mechanics within the MOE, and the generalized Born/Volume integral implicit solvent model of the MOE was used for solvation energy estimation [29]. The binding free energies of the anesthetics,  $\Delta G_{\text{bind}}$ , were estimated using the db\_DockScore program (MOLSIS Inc., Japan) [30] to calculate GBVI/WSA\_dG (Generalized-Born Volume Integral/Weighted Surface Area), a scoring function of MOE docker [31] from the complex structure, which uses the molecular mechanics force field on the MOE platform. Amobarbital, (*R*)-pentobarbital, (*S*)-pentobarbital, etomidate, propofol, halothane, isoflurane, sevoflurane, and desflurane were docked flexibly to the 6i53 model to determine the binding site of GABA<sub>A</sub>R.

### Analysis of Binding Interactions

The molecular interactions between GA molecules and their binding sites were analyzed and represented using ligand interaction diagrams in the MOE [32].

### Hydration Water Molecule Analysis of the TMD and Intersubunits

The distribution of hydration water molecules of the TMD was examined using the TMD (M1-M2-M3) model. The water oxygen density of the model was calculated using the 3D-RISM theory method [21], which includes solvent analysis in the MOE [26]. Hydration water molecules were visualized by the water-mapping method in the MOE using the obtained water oxygen density [26]. To examine the change in the distribution of hydration water molecules with and without propofol binding, the water oxygen density of the propofol-TMD model complex was calculated.

For intersubunit hydration, the oxygen density of the hydration water molecules of the dimer models, that is, of  $\alpha_1/\beta_3$ ,  $\beta_3/\alpha_1$ ,  $\gamma_2/\beta_3$ ,  $\alpha_1/\gamma_2$  subunit dimers, was calculated. Next, the oxygen density of the sevoflurane binding dimers was calculated within 20 Å of the sevoflurane molecule. The hydration water molecules of the GA-dimer complex were visualized using the water-mapping method. Water-mapping was performed by limiting it to within 8 Å of the GA molecule, where significant changes in distribution were observed. Changes in the water molecule distribution with and without GA molecules were examined. Changes in the water distribution with and without GA binding were analyzed.

## Results

### GA Binding Sites of GABA<sub>A</sub> Receptor

ASEDock molecular docking was used to search for binding sites covering the entire 3D structure and to rank the binding sites in order of the docking score. Multiple binding sites were found, and the propofol #9 site in the  $\alpha_1/\beta_3$  intersubunit had the highest score among the intersubunit sites. Propofol #11 and #14 sites within the  $\beta_3/\alpha_1$  and  $\gamma_2/\beta_3$  intersubunit, followed respectively. At the propofol #11 site, propofol was bound to the  $\beta_3/\alpha_1$  intersubunit TMD, a typical GA-binding site (Figure 3A). Propofol in #11 of the  $\beta_3/\alpha_1$  intersubunit was surrounded by helices of  $\beta_3$ M2-  $\beta_3$ M3- $\alpha_1$ M1 and interacted with T262 (Thr) of  $\beta_3$ M2 and F289 (Phe) of  $\beta_3$ M3 via hydrogen and  $\pi$ - $\pi$  bonds, respectively (Figure 3B).



The binding residue at the propofol #11 site was consistent with the results obtained by photolabeling [9]. The propofol binding sites of the  $\alpha_1/\beta_3$ ,  $\beta_3/\alpha_1$  and  $\gamma_2/\beta_3$  intersubunits of the GABA<sub>A</sub> receptor were reproduced using the ASEDock [11].

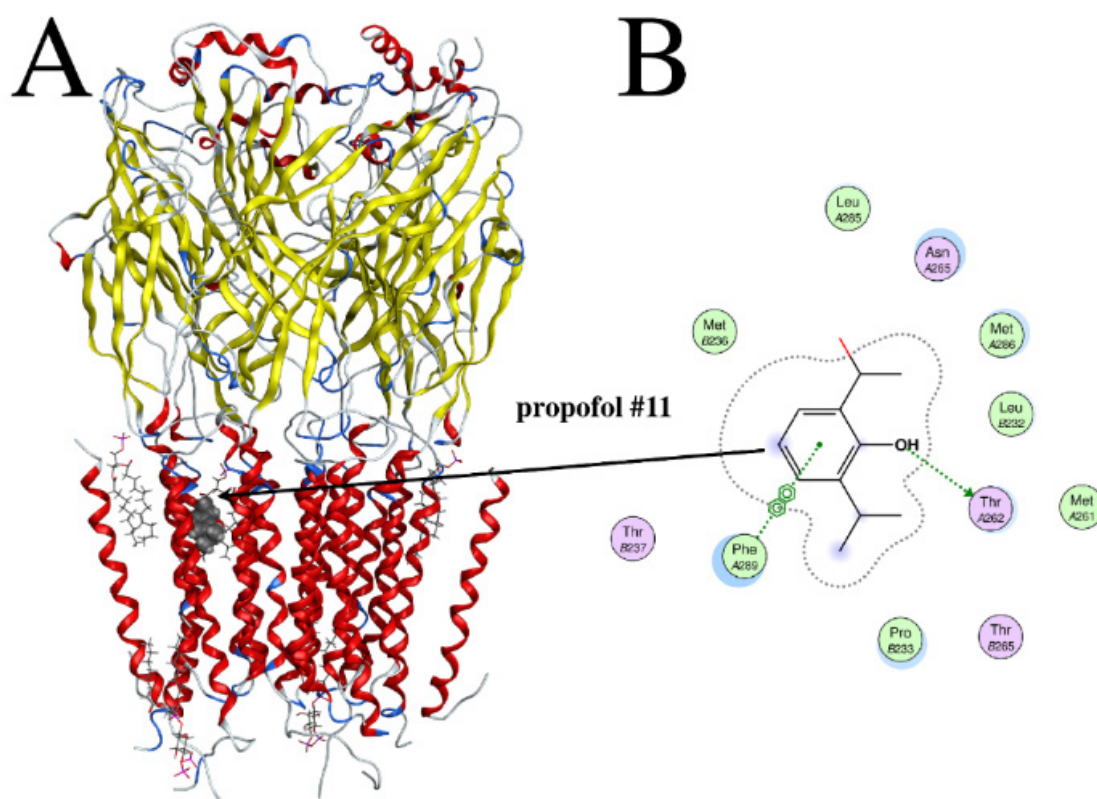


**Figure 3** **A:** Propofol #11 binding site in  $\beta_3/\alpha_1$  intersubunit transmembrane domain (TMD) of GABA<sub>A</sub> receptor (PDB ID: [6i53](#)) found by ASEDock. **B:** Binding interactions at propofol #11 site analyzed using ligand interaction diagram in MOE. Residue, chain, A( $\beta_3$ ) or B( $\alpha_1$ ), and number, respectively. Hydrogen bond to  $\beta_3$  Thr262 and  $\pi$ - $\pi$  bond to  $\beta_3$  Phe289 are seen.

ASEDock output selected for intersubunit GA binding sites is shown in the binding site rank. The binding free energy of GA, ( $\Delta G_{\text{bind}}$ ), was calculated from the molecular interactions between the GA molecule and its binding sites using the db\_DockScore program. The binding sites and  $\Delta G_{\text{bind}}$  values of the  $\alpha_1\beta_3\gamma_2$  GABA<sub>A</sub>R intersubunit are shown (Table 1). The highest ranking binding sites of GAs were found in the  $\beta_3/\alpha_1$  intersubunit, with the exception of the propofol site. GAs selectively bind to the  $\beta_3/\alpha_1$  intersubunit. Ranking is based on the docking score that reproduces the ligand-receptor complex structure in the crystal field. The binding free energy was derived from the binding reaction in the aqueous phase. Strictly speaking, the definition of the binding site is different in the crystal field and aqueous phases. The binding sites specified by ranking are not necessarily the most stable in binding free energy. GAs have diverse molecular structures, such as barbital, phenol, hydrocarbon, and ethers. Even with various structures, GAs were found to bind selectively to the  $\beta_3/\alpha_1$  intersubunit, the common GA binding site.

### Hydration of Intersubunits

Five  $\alpha_1$ ,  $\beta_3$ , and  $\gamma_2$  subunits (A, B, C, D, and E chains) and four of the five intersubunits, namely  $\beta_3/\alpha_1$  (ED, BA),  $\gamma_2/\beta_3$  (CB),  $\alpha_1/\beta_3$  (AE), and  $\alpha_1/\gamma_2$  (DC), are associated with the formation of a pentamer in a circumferential shape. Two  $\beta_3/\alpha_1$  inter-subunits, the ED and BA chains, were identified (Figure 2A, 2B). The oxygen atom density of the TMD (M1-M2-M3) model was calculated using the 3D-RISM method, and the distribution of hydration water molecules was investigated (Figure 4A and 4C). The binding site of the hydration water molecule (within 8 Å of the propofol molecule) was determined on the basis of the presence or absence of propofol binding. The hydration change of the  $\beta_3/\alpha_1$  (ED) intersubunit TMD with and without #11 propofol binding is shown in Figure 4.

**Table 1** General anesthetic binding rank and binding free energy of intersubunit site of  $\alpha_1\beta_3\gamma_2$  GABA<sub>A</sub> receptor

intersubunit chain composition <sup>†</sup> general anesthetic <sup>§</sup>	$\beta_3/\alpha_1$		$\gamma_2/\beta_3$		$\alpha_1/\beta_3$		$\beta_1/\gamma_2$			
	ED rank <sup>‡</sup>	BA $\Delta G_{\text{bind}}/\text{kcal}^{-1}$	CB rank <sup>‡</sup>	AE $\Delta G_{\text{bind}}/\text{kcal}^{-1}$	DC rank <sup>‡</sup>	DC $\Delta G_{\text{bind}}/\text{kcal}^{-1}$	DC rank <sup>‡</sup>	DC $\Delta G_{\text{bind}}/\text{kcal}^{-1}$		
amob	#10	-7.1	#33	-7.3	#342	-6.9	#48	-6.3	#42	-6.9
( <i>r</i> )-pento	#6	-6.9	#9	-6.7	#822	-7.3	#186	-6.5	#78	-6.0
( <i>s</i> )-pento	#4	-7.1	#12	-6.9	#155	-6.6	#183	-6.5	#15	-6.3
etomi	#3	-7.6	#31	-6.5	#48	-6.8	#84	-6.3	#85	-5.8
prop	#11	-6.0	#45	-5.8	#14	-6.1	#9	-6.3	#30	-5.2
halo	#1	-4.1	#2	-4.1	#35	-4.5	#12	-4.1	#9	-3.9
isof	#12	-4.7	#10	-4.7	#200	-4.8	#23	-4.7	#34	-4.5
sevo	#3	-4.9	#4	-4.9	#69	-5.1	#13	-4.9	#80	-4.2
desf	#27	-4.4	#6	-4.5	#141	-4.7	#13	-4.3	#32	-4.2

<sup>†</sup>Sequence chain of intersubunit: A-E. <sup>‡</sup>rank: the binding site in a score order of ASEDock.  $\Delta G_{\text{bind}}$ : binding free energy of GA with 2.1 kcal mol<sup>-1</sup> of mean unsigned error. <sup>§</sup>amob (amobarbital), (*R*)-pento (*R*-pentobarbital), (*S*)-pento (*S*-pentobarbital), etomi (etomidate), prop (propofol), halo (halothane), isof (isoflurane), sevo (sevoflurane), desf (desflurane).

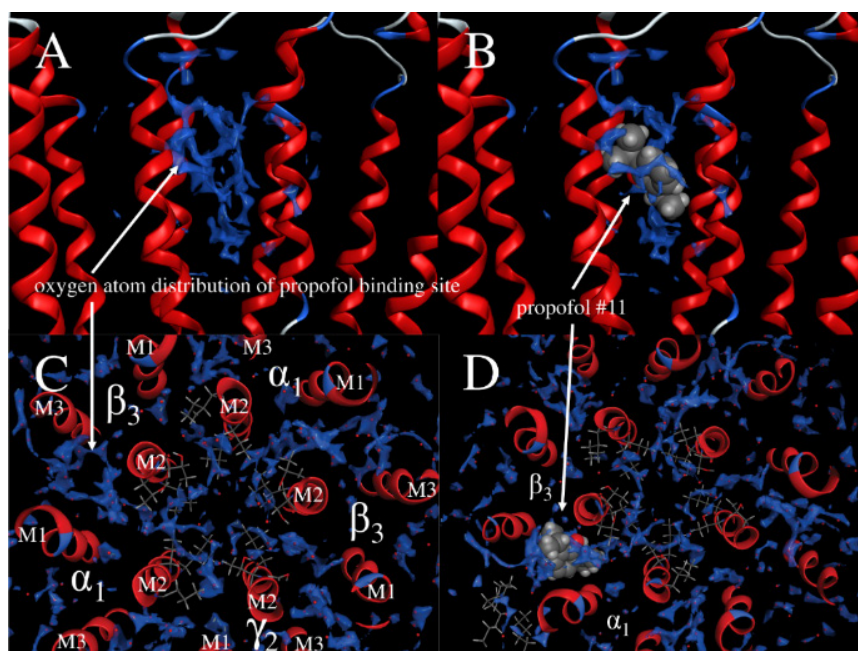


**Figure 4** Isopycnic surface of hydration oxygen distribution at bulk water density with and without propofol binding calculated using 3D-RISM. **A, C**: extracellular and side views of  $\alpha_1\beta_3\gamma_2$  GABA<sub>A</sub> receptor transmembrane domain (TMD). TMD model:  $\alpha_1$  subunit: 224-318 residue of A-chain,  $\beta_3$ : 219-308 of B-chain,  $\gamma_2$ : 224-323 of C-chain,  $\alpha_1$ : 224-313 of D-chain and  $\beta_3$ : 219-308 of E-chain. Each subunit is consisted of M1-M2-M3 helices in the model. Five M2 helices in the center form the channel conduit. **B, D**: GABA<sub>A</sub> receptor TMD with propofol #11. The propofol bound to  $\beta_3/\alpha_1$  intersubunit, i.e., to the hydration duct, which continues to the channel conduit of the receptor.

The hydration arrangements of dimer models,  $\beta_3/\alpha_1$  (ED, BA),  $\gamma_2/\beta_3$  (CB),  $\alpha_1/\beta_3$  (AE), and  $\alpha_1/\gamma_2$  (DC), were analyzed from the water oxygen density using the water-mapping method within 8 Å of the binding sevoflurane molecule.  $\Delta N$  and  $\delta$  denote dehydration numbers of sevoflurane binding process and of the binding site, respectively. The sevoflurane-binding site of each intersubunit contained 19-24 molecules of hydration number ( $N_{\text{site}}$ ). Sevoflurane molecules have a hydration of 8.83 water molecules ( $N_{\text{sevo}}$ ). The binding site-sevoflurane complex has hydration of 15-19 water molecules ( $N_{\text{SGA}}$ ). (Table 2).  $\Delta N$  and  $\delta$  have intersubunit dependency correlated with ASEDock rank. The hydration number of the sevoflurane site and the complex ( $N_{\text{site}}$ ,  $N_{\text{SGA}}$ ) did not show rank dependency. The protein hydration layer was analyzed using water-mapping. First layer water molecules and gap water molecules (second layer, contact layer molecules)

**Table 2** Hydration and dehydration numbers of sevoflurane binding site of intersubunits

intersubunit	$\beta_3/\alpha_1$		$\gamma_2/\beta_3$	$\alpha_1/\beta_3$	$\alpha_1/\gamma_2$
chain composition†	ED	BA	CB	AE	DC
rank‡	#3	#4	#69	#13	#80
total dehydration ( $\Delta N$ )§	13.87	13.22	12.66	13.27	12.67
$\delta(N_{\text{site}}-N_{\text{SGA}})$ §	5.34	4.69	4.13	4.74	4.14
binding site ( $N_{\text{site}}$ )§	24.06	21.04	23.52	19.52	20.69
first layer water	12.57	10.51	12.53	10.28	6.65
gap water (other)	11.49	10.53	10.99	9.24	14.04
sevoflurane ( $N_{\text{sevo}}$ )§	8.53	8.53	8.53	8.53	8.53
binding complex ( $N_{\text{SGA}}$ )§	18.72	16.35	19.39	14.78	16.55
first layer water	12.30	9.14	9.72	8.27	4.53
gap water (other)	6.42	7.21	9.67	6.51	12.02

†Sequence chain of intersubunit: A-E. ‡rank: the binding site by docking in a stable order. §  $\Delta N$ : dehydration number of sevoflurane binding process,  $\delta$ : dehydration number of the binding site.  $N_{\text{site}}$ : hydration number of sevoflurane binding site,  $N_{\text{sevo}}$ : hydration number of sevoflurane molecule, and  $N_{\text{SGA}}$ : hydration number of the binding complex.

numbers in  $N_{\text{site}}$  and  $N_{\text{SGA}}$  are shown. Dehydration of the  $\beta_3/\alpha_1$  and  $\alpha_1/\beta_3$  intersubunits by sevoflurane binding originated mainly from the gap water of the intersubunit hydration.

The hydration arrangement of the  $\beta_3/\alpha_1$  (ED) dimer model was analyzed from the water oxygen density within 8 Å of the binding GA molecule using the water-mapping method. For all GA molecule in  $\beta_3/\alpha_1$  intersubunit (ED) the hydration numbers are listed in Table 3. The GA binding site of the intersubunit contained 21-33 molecules of hydration number ( $N_{\text{site}}$ ) depending on the GA molecule size. GA molecules have hydration of 6-9 water molecules ( $N_{\text{GA}}$ ). The binding site-sevoflurane complexes have hydration of 16-25 water molecules ( $N_{\text{SGA}}$ ).

**Table 3** Hydration and dehydration numbers of general anesthetic (GA) binding site of  $\beta_3/\alpha_1$  intersubunit (ED)

general anesthetic§	$\Delta G_{\text{bind}}/\text{kcal mol}^{-1}\dagger$	$N_{\text{site}}\ddagger$	$N_{\text{GA}}$	$N_{\text{SGA}}$	$\Delta N$	$\delta$
amob#10	-7.13	32.58	9.51	24.10	17.99	8.48
( <i>R</i> )-pento#6	-6.94	30.76	9.49	24.65	15.60	6.11
( <i>S</i> )-pento#4	-7.10	27.16	8.18	19.86	15.48	7.30
etomi#3	-7.63	31.26	6.44	21.04	16.66	10.22
prop#11	-6.04	26.37	9.49	24.65	15.26	1.72
halo#1	-4.14	21.66	4.71	16.45	9.92	5.21
isof#12	-4.66	21.41	6.22	18.12	9.51	3.29
sevo#3	-4.93	24.06	8.53	18.72	13.87	5.34
desf#27	-4.40	22.31	6.16	18.43	10.04	3.88

† $\Delta G_{\text{bind}}$ : binding free energy of GA with 2.1 kcal mol<sup>-1</sup> of mean unsigned error. ‡ $N_{\text{site}}$ : hydration number of GA binding site,  $N_{\text{GA}}$ : hydration number of GA molecule,  $N_{\text{SGA}}$ : hydration number of the binding complex,  $\Delta N$ : dehydration number of GA binding process,  $\delta$ : dehydration number of GA binding site ( $N_{\text{site}}-N_{\text{SGA}}$ ). §amob (amobarbital), (*R*)-pento ((*R*)-pentobarbital), (*S*)-pento ((*S*)-pentobarbital), etomi (etomidate), prop (propofol), halo (halothane), isof (isoflurane), sevo (sevoflurane), desf (desflurane).

### Hydration of GABA<sub>A</sub> Receptor

The relationship between the water distribution of the channel conduit and the hydration distribution of the intersubunit was investigated using the TMD (M1-M2-M3) structural model. The channel conduit through which the ions pass inside the cylinder is surrounded by five M2 helices (Figure 2A, 2B). A sliced  $\alpha_1\beta_3\gamma_2$  GABA<sub>A</sub>R shows the hydrophobic gate of M2 Leu 9' perpendicular to the conduit (Figure 5) [8]. The oxygen atom densities were found to be distributed radially from the central channel conduit (M2 9'-16') to the intersubunit in five directions. Hydration water was found to be continuously distributed from the conduit to the intersubunit, resulting in the formation of a water duct.



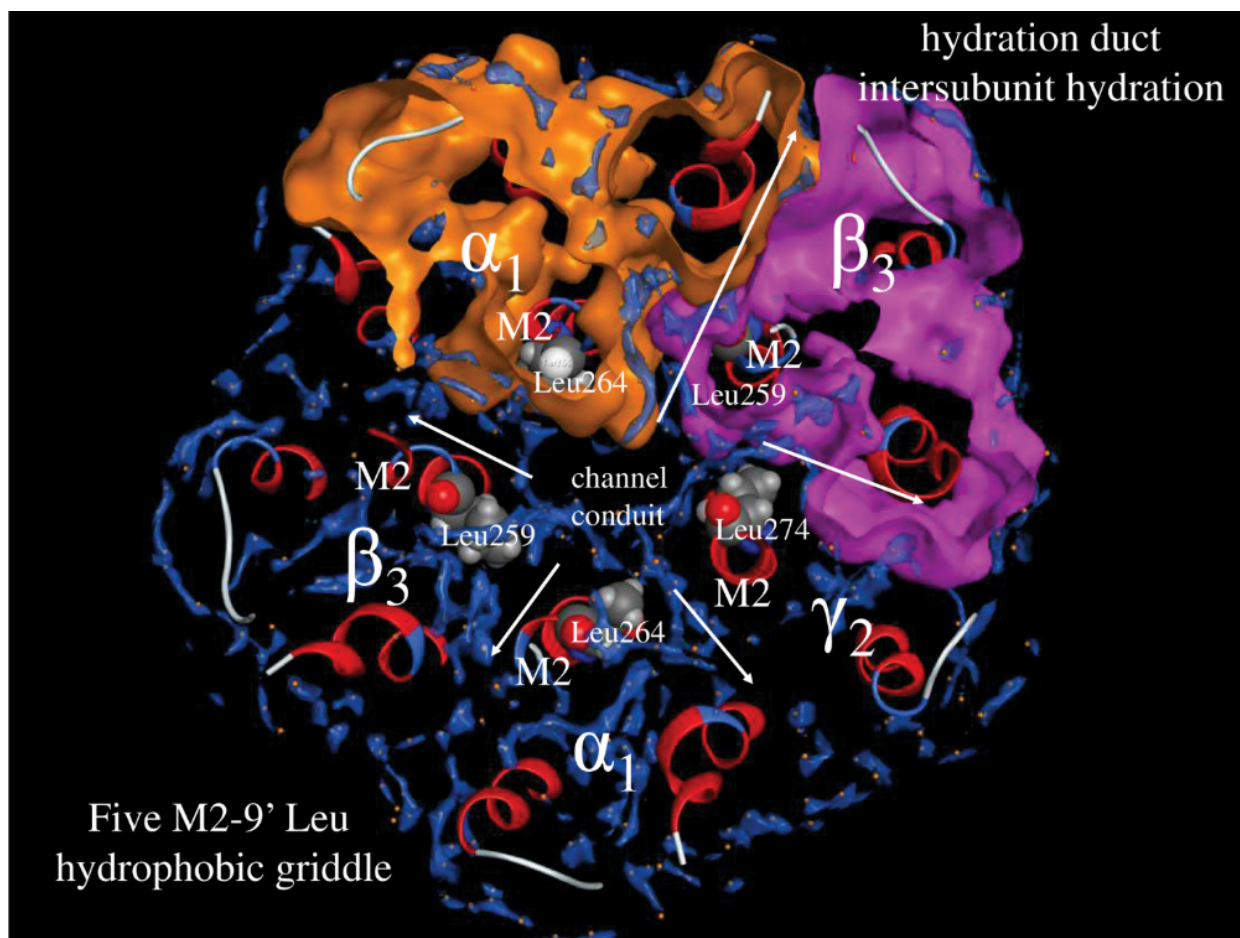


**Figure 5**  $\alpha_1\beta_3\gamma_2$  GABA<sub>A</sub> receptor (TMD model of PDB ID: [6i53](#)): M2 6'-16' slice view parallel to the membrane. Isopycnic surface of oxygen atom distribution at bulk water density in the M2 6'-16' slice (blue) calculated using 3D-RISM. The molecular surfaces of the  $\beta_3$  (magenta) and  $\alpha_1$  (orange) subunits are shown. Five directional radial distributions of intersubunit hydration continued to the channel conduit of GABA<sub>A</sub> receptor. The hydrophobic griddle of five M2-9' Leu (CPK model) of the duct is shown.

#### Dehydrations of Intersubunits due to Propofol and Sevoflurane Binding

The dehydration numbers within 8 Å of the binding propofol molecule before and after binding were compared using dimer models. Binding of propofol to the  $\beta_3/\alpha_1$  intersubunit occurs via hydration and dehydration (Figure 4). In addition, propofol binding disrupted the hydration of water and changed the distribution of water in the duct (Figure 4C, 4D; Figure 5).

Next, the hydration numbers within 8 Å of the binding sevoflurane molecule before and after binding were compared (Table 2; Figure 6) using the  $\beta_3/\alpha_1$  model. Dehydration of approximately five water molecules was observed in the  $\beta_3/\alpha_1$  (ED),  $\beta_3/\alpha_1$  (BA), and  $\alpha_1/\beta_3$  (AE) intersubunits. The dehydration of the intersubunit was approximately 4-5%.

#### GA Binding Free Energy Correlated to Dehydration and Hydration Numbers at the Binding Site of $\beta_3/\alpha_1$ (ED) Intersubunit

The hydration and dehydration numbers of the GA binding site of the  $\beta_3/\alpha_1$  intersubunit are shown in Table 3.  $\Delta G_{\text{bind}}$  of the binding free energy was compared with the hydration number of the GA binding site within 8 Å from the GA molecule ( $N_{\text{site}}$ ), hydration number of the GA molecule ( $N_{\text{GA}}$ ), hydration number of the binding complex ( $N_{\text{SGA}}$ ), dehydration number of the GA binding process ( $\Delta N$ ), and the dehydration number of GA binding sites ( $\delta$ ,  $N_{\text{site}} - N_{\text{SGA}}$ ).  $N_{\text{site}}$  indicates the hydration number of the site prior to binding.

The GA binding free energy  $\Delta G_{\text{bind}}$  correlated with the dehydration number of the GA binding process  $\Delta N$  and hydration number of the binding site  $N_{\text{site}}$  at the  $\beta_3/\alpha_1$  (ED) intersubunit binding site (Figure 7;  $r^2 = 0.88$ ,  $0.84$ , respectively). In contrast, the dehydration number of the GA binding site ( $\delta$ ) was poorly correlated with  $\Delta G_{\text{bind}}$  ( $r^2=0.48$ ).



Seto: General anesthetic binding via hydration

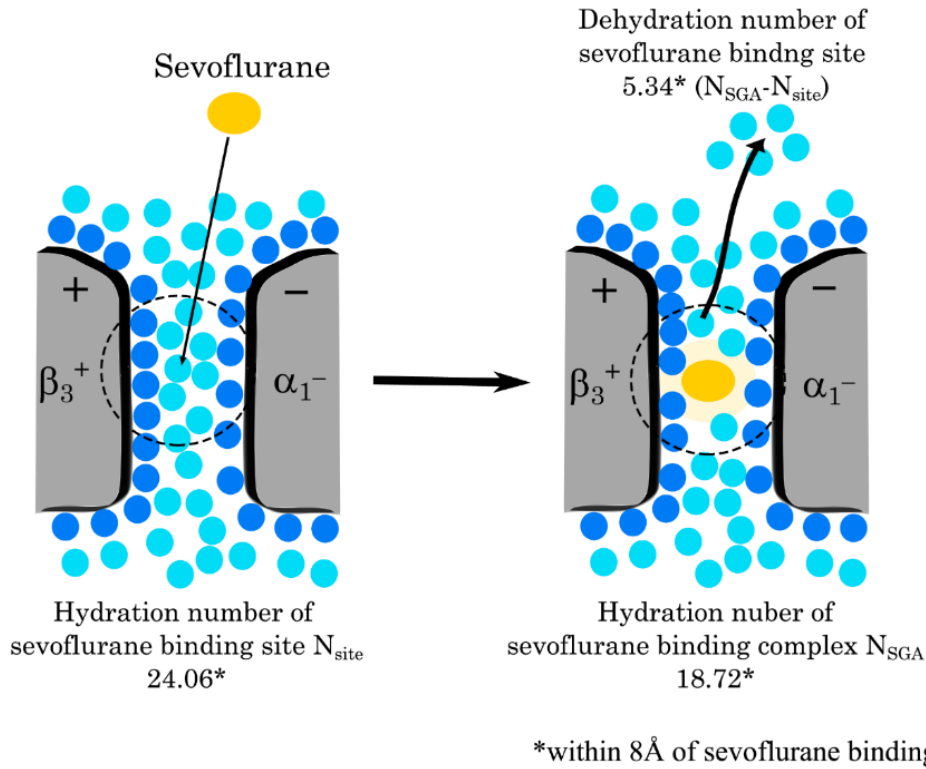


**Figure 6** Dehydration of the  $\beta_3^+/\alpha_1^-$  intersubunit transmembrane domain due to sevoflurane binding. 5.34 water molecules were dehydrated from the intersubunit hydration under the conditions of hydration distribution within 8 Å of binding sevoflurane molecule.

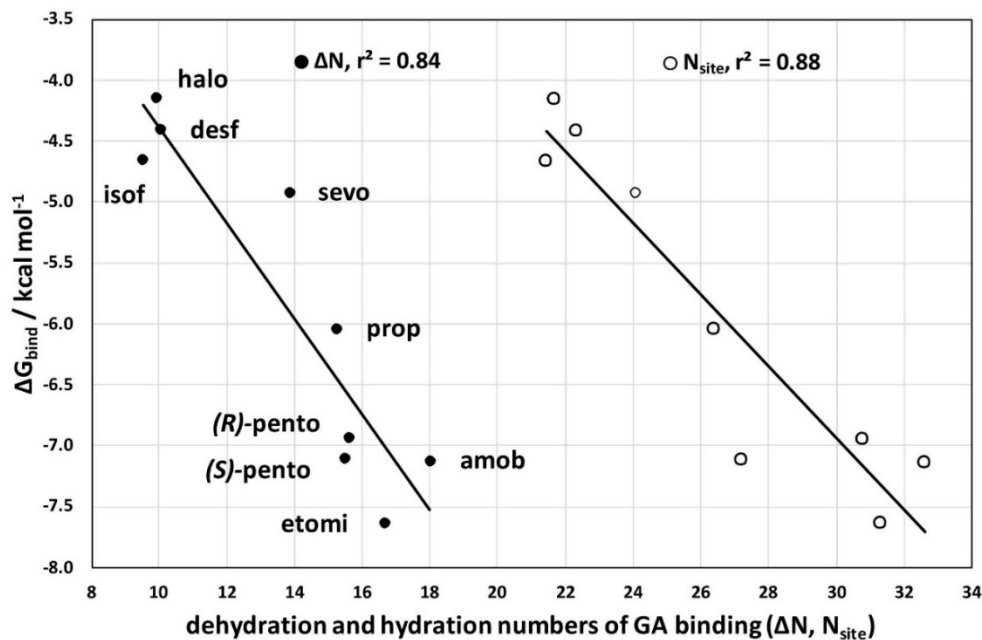


**Figure 7** Correlation of binding free energy to the dehydration and hydration numbers of the binding site. Binding free energy of general anesthetics,  $\Delta G_{\text{bind}}$ , dehydration number of binding process ( $\Delta N$ ) and hydration number of the binding site of  $\beta_3/\alpha_1$  intersubunit ( $N_{\text{site}}$ ). amob (amobarbital), (R)-pento ((R)-pentobarbital), (S)-pento ((S)-pentobarbital), etomi (etomidate), prop (propofol), halo (halothane) isof (isoflurane) sevo (sevoflurane), desf (desflurane)

## Discussion

### ASEDock and $\Delta G_{\text{bind}}$ Validity

A discussion based on these predicted structures should have certain limitations in the ASEDock program. The accuracy of structure prediction is highly dependent on the ligand-conformer generating algorithm, fitting search algorithm, electrical charges, force fields, etc. The ASEDock program was confirmed to have 80% reproducibility within the estimated experimental error using 59 high-quality X-ray structures of the complexes [19]. Predictive results have been carefully accepted by conducting ex post facto verification in this field.

The validity of GBVI/WSA\_dG was verified by comparison with the experimental  $\Delta G$  using the CSAR-NRC HiQ dataset (343 ligand-protein complexes). GBVI/WSA\_dG has 2.09 kcal mol<sup>-1</sup> of mean unsigned error and 2.73 kcal mol<sup>-1</sup> of root mean square error with  $R^2 = 0.30$  [31].

### Dehydration of Binding Process in $\beta_3/\alpha_1$ Intersubunit (ED) Stabilizes GA Binding Free Energy

The dehydration number of the GA binding process ( $\Delta N$ ) was well correlated with the binding free energy of GA ( $\Delta G_{\text{bind}}$ ) (Figure 7, left,  $r^2=0.84$ ). The higher the dehydration number ( $\Delta N$ ), the more stable  $\Delta G_{\text{bind}}$  is.  $\Delta G_{\text{bind}}$  was found to be related to dehydration from hydration rearrangements during the binding process. The hydration number of the GA binding site ( $N_{\text{site}}$ ) correlated with the binding free energy of GA ( $\Delta G_{\text{bind}}$ ) (Figure 7, right,  $r^2=0.88$ ). The higher the hydration number ( $N_{\text{site}}$ ), the more stable  $\Delta G_{\text{bind}}$ .  $\Delta G_{\text{bind}}$  is found to relate to the hydration state of the binding site. The GA hydration number ( $N_{\text{GA}}$ ) and dehydration number of the binding site ( $\delta$ ) did not correlate with  $\Delta G_{\text{bind}}$ . Neither  $N_{\text{GA}}$  nor  $\delta$  alone was related to  $\Delta G_{\text{bind}}$ . The dehydration number of the GA binding process  $\Delta N$  is due to both hydration rearrangements of the intersubunit binding site and from dehydration of the GA molecule. The GA binding free energy  $\Delta G_{\text{bind}}$  is stabilized by both the hydration rearrangement of the inter-subunit binding site and dehydration of the GA molecule. In addition, the higher the hydration number of the GA binding site  $N_{\text{site}}$  in the pre-binding state, the more stable  $\Delta G_{\text{bind}}$  is. Both the dehydration during the binding process and the pre-binding hydration state were involved in  $\Delta G_{\text{bind}}$ . Investigation of water molecule numbers of the GA binding site revealed that the hydration rearrangements of GA binding sites and GA molecules are involved in GA binding of the  $\beta_3/\alpha_1$  intersubunit of GABA<sub>A</sub>R. We clarified that the hydrations are involved in the GA binding of GABA<sub>A</sub>R.

### GA Binding Process to Intersubunit Site can be Regarded as a Dissolution Process into Interfacial Water of the Intersubunit Binding Site

The dissolution process of nonpolar substances (nps) can be broken down into three processes: (1) void formation, (2) transfer to the void, and (3) solute-solvent interactions in the thought experiment (Figure 8A) [33,34]. The energy change estimation for each process provided an understanding of the origin of the dissolution free energy. Analysis by scaled particle theory suggests that the major component of the dissolution free energy is void formation[34]. Void formation (bulk water exclusion) corresponds to the reversal of the void hydration process.

Since hydration of the intersubunit binding site of GABA<sub>A</sub>R and GA are involved in the GA binding process, we thought that the GA binding process can be regarded as a dissolution process in the interfacial water of the binding site, following nonpolar substance (nps) dissolution. Similar to nps dissolution, the GA binding process can be decomposed into (1) void formation at the binding site (interfacial water exclusion), (2) GA transfer to the void, and (3) GA-interface water interactions (Figure 8B). Although this decomposition is an arbitrary thought experiment, the GA binding process can be regarded as the GA dissolution process in the interfacial water of the GA binding site, and the dehydration number of the GA binding process  $\Delta N$  can be understood as a consequence of the interfacial water molecule exclusion. The GA binding process can be understood as the dissolution process into interfacial water of the binding site.

### Binding Interactions of GA Binding Mode via Hydration

In general, drugs are designed to avoid side effects and exert specificity, and are developed by selecting drugs with highly specific key and keyhole molecular recognition [35]. The molecular interactions of drugs at their binding sites are both directional and structure-dependent interactions (i.e., dependent on electrostatic interactions, hydrogen bonds, and van der Waals interactions). In addition, GAs exhibit a binding mode characterized by the involvement of hydration water.

The GA molecule in the binding site directly interacts with the binding site (Figure 3B) and contacts the hydrated water molecules (Figure 4B, 4D). Presumably, binding GA molecules have electrostatic and van der Waals interactions with hydrated water molecules at the binding site. Since the water molecule has a dipole, dipole interactions may also occur in the GA-binding site. The GA direct interactions in the binding site have an anisotropy that depends on the shape of the GA molecule. On the other hand, hydrated water molecules are considered to bring about isotropic interactions with electrostatic and van der Waals interactions that average out the anisotropy interactions from thermal fluctuations. The binding free energy is related to the dehydration number during the binding process and the binding site hydration number before binding, rather than to the shape of the GA molecule (Figure 7).

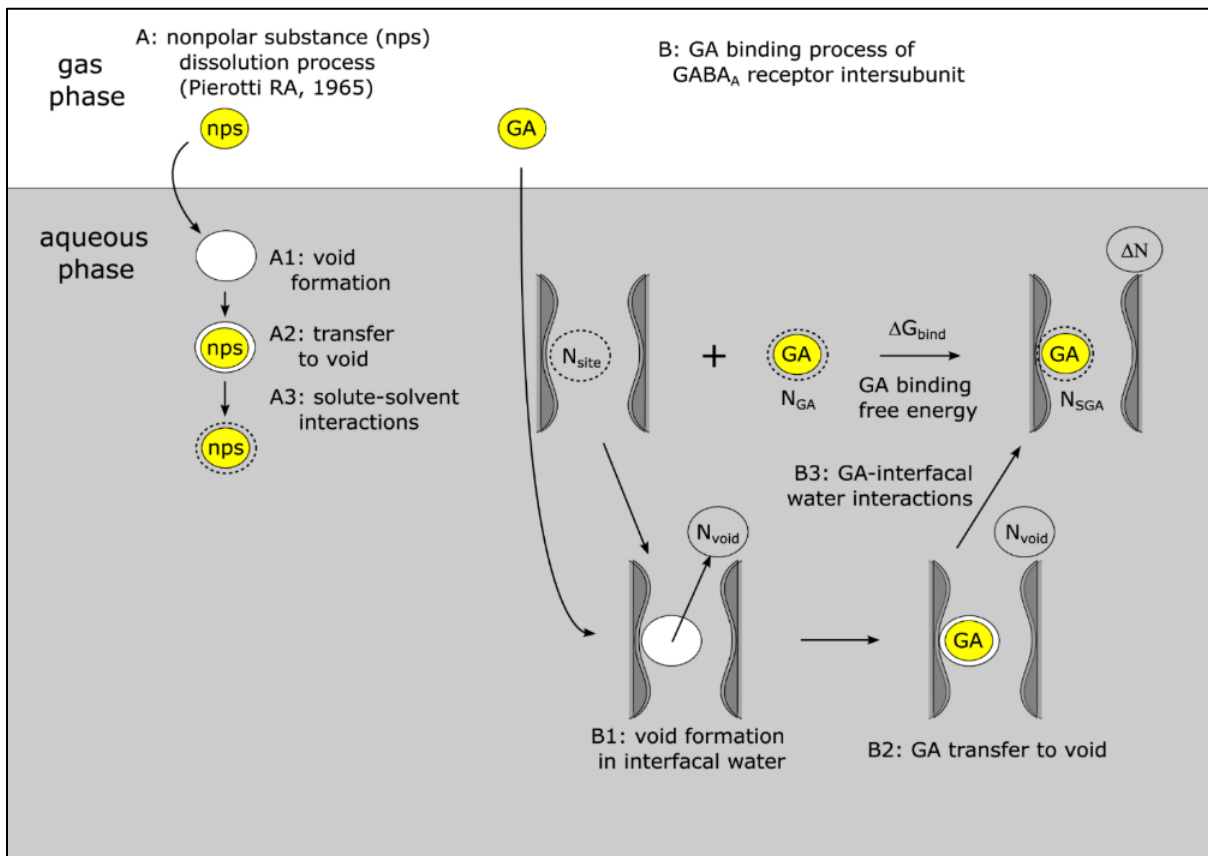


**Figure 8** **A:** Nonpolar substance (nps) dissolution process. A1: void formation. A2: transfer to void. A3: solute-solvent interactions. **B:** GA binding process of GABA<sub>A</sub> receptor intersubunit. B1: Void formation in interfacial water. B2: GA transfer to void. B3: GA-interfacial water interactions.  $N_{site}$ : hydration number of GA binding site,  $N_{GA}$ : hydration number of GA molecule,  $N_{SGA}$ : hydration number of the binding complex,  $\Delta N$ : dehydration number of GA binding process.

### The Characteristics of General Anesthesia and GA Binding Mode via Hydration

The characteristics of GA include (1) weak binding affinity [13], (2) affinity with the binding site correlating with solubility in olive oil rather than molecular shape [14], and (3) weak steric discrimination of optical isomeric anesthetics, have been pointed out [15]. The binding affinities of GA and common drug were compared using half-effect concentrations ( $EC_{50}$ ). Encorafenib, an anti-malignant tumor growth agent BRAF inhibitor, shows an  $EC_{50}$  of 40 nmol/l or less [36], while propofol and sevoflurane show an  $EC_{50}$  of approximately 2 and 330  $\mu\text{mol/l}$ , respectively [37]. Generally, we recognize that GA binding affinities tend to be weaker than those of other drugs. The binding sites of GA with diverse chemical structures have been revealed to be  $\beta_3/\alpha_1$  and  $\alpha_1/\beta_3$   $\gamma_2/\beta_3$  intersubunits for propofol [9],  $\beta_3/\alpha_1$  intersubunit for etomidate [12], and  $\beta_3/\alpha_1$  and  $\alpha_1/\beta_3$  intersubunits for volatile anesthetics (VAs: halothane, isoflurane, sevoflurane) [10] from photolabeling experiments.

Regarding the binding site reproducibility by docking, we consider that the GA binding site does not necessarily have to reproduce it at the residue level, but that the reproducibility at the intersubunit level is sufficient because hydration is involved. In this study using ASEDock, the binding sites of propofol, etomidate, and VAs reproduced the results of a previous study using photolabeling. However, the barbiturate-binding sites did not always agree with the photolabeling results [15]. Generally, the docking results reproduced GA binding sites with various structures in the intersubunit (Table 1) and showed that GA molecular discrimination was weak, thus reproducing the characteristics of GA.

Distribution analysis of hydration water molecules by water-mapping clarified that GA binding occurs via hydration. GA-binding site interactions may occur via bipolar and van der Waals interactions of hydration water molecules. One reason for the weak affinity of GA is thought to be that the GA-binding site distance increases because of hydration compared with direct interactions. In GA-binding site interactions, the anisotropic interactions dependent on the shapes of the GA molecule and the binding site are averaged out by the thermal fluctuation of the hydration water. Binding interactions could occur even if the molecular shape does not fit the site, which can be explained by the binding mode via hydration. The mechanism showing the characteristics of GA is understood from hydrations at the binding site.

### Sevoflurane Binding Selectivity to the $\beta_3/\alpha_1$ Intersubunit

The pharmacological actions of GA binding in the GABA<sub>A</sub>R intersubunit have been shown to depend on the subunit constitution of the receptor [9]. However, how GAs discriminate various intersubunit spaces remains a question [38].

Table 2 shows the intersubunit selectivity of sevoflurane binding. In this study, we evaluated the intersubunit selectivity from the correlation with ASEDock rank. The sevoflurane docking rank was confirmed to reproduce the binding to the  $\beta_3/\alpha_1$  and  $\alpha_1/\beta_3$  intersubunits identified by photolabeling sevoflurane, which has an anesthetic effect [10]. ( $\Delta G_{\text{bind}}$  had a mean unsigned error of 2.1 kcal mol<sup>-1</sup>.  $\Delta G_{\text{bind}}$  is useful for evaluating binding affinity with a dynamic range beyond this, but for evaluations within the error, such as intersubunit selectivity, it cannot be used.)  $\Delta N$  and  $\delta$  are correlated with the intersubunit selectivity by rank.  $\Delta N$  is the sum of the dehydration numbers of the sevoflurane-binding process, i.e., the dehydration number of the sevoflurane-binding site and the dehydration number of sevoflurane hydration. In addition to the correlation of  $\Delta N$ , the correlation of  $\delta$  alone was also observed; therefore, the main component of  $\Delta N$  was  $\delta$ . Dehydration of sevoflurane binding is considered to cause intersubunit selectivity.

$\Delta N$  and  $\delta$  depend on the ease of intersubunit dehydration (stability of intersubunit hydration) rather than shape fitting, which causes the sevoflurane molecule to interact with specific amino acid residues in the binding site. (Table 2, Figure 7). Protein hydration can be classified into the first, second, and contact layers [39]. The ease of dehydration of the first and second layers of intersubunit binding water is determined by the hydration state of the binding site.

Depending on the subunit composition, various intersubunits exist in the GABA<sub>A</sub> receptor. This study revealed that the  $\beta_3/\alpha_1$  and  $\alpha_1/\beta_3$  intersubunit selectivity of sevoflurane binding depends on the ease of dehydration of sevoflurane binding (Table 2). Due to the involvement of hydration in GA binding, even the same GA can have different docking ranks when the dehydration number in the binding process is different. Dehydration of the sevoflurane binding process may explain the different pharmacological effects depending on the subunit composition.

### GA Binding may Affect Subunit Fluctuation and the Open-close Transition of the Channel

GABA<sub>A</sub>R consists of a subunit pentamer, wherein the surfaces of the subunit associations are complementary and loosely bound. The first layer of hydration is surface water, which is directly hydrogen-bonded to the subunit surface atoms. The second layer is a water molecule in which hydrogen bonds with the first layer of hydration. The third and subsequent layers are called contact layers, wherein water molecules mediate intersubunit interactions [39]. The subunit fluctuation could be transmitted to the opposite subunit through the layers of hydration and is considered to be related to the open-close transition of the GABA<sub>A</sub>R channel. When hydration water is confined to a region of approximately 9 Å in the channel conduit, a gas-liquid phase transition occurs stochastically. Water molecules in the gas phase dissipate, creating a barrier to ion conduction in the conduit. The opening and closing of the channel due to the gas-liquid phase transition is known as hydrophobic gating [40,41]. In GABA<sub>A</sub>R, there is a hydrophobic grid at M2 Leu 9' of the channel conduit, which constitutes a hydrophobic gate (Figure 5) [8]. From the results of 3D-RISM in this study, a continuous hydration density was observed from the channel conduit to the intersubunit duct in five radial directions at the height of the 16' residue (Figure 4C, Figure 5). Propofol was found to bind to the intersubunit of  $\beta_3$ -Thr262 at the M2 12'-residue (Figure 4D), blocking the distribution of hydration water molecules in the intersubunit duct. We speculate that propofol binding reconstituted intersubunit hydration, suggesting that intersubunit hydration changes may affect hydrophobic gating by wetting-dewetting of channel conduits.

### Proposal of Hydration Voidance Hypothesis of Interfacial Water: beyond the Electro-restricted Water Release Hypothesis

In the hypothesis of electro-restricted water release for general anesthesia [42], the site of action of the anesthetic is the water interface, wherein the binding of the anesthetic results in the release of electro-restricted water around the polar amino acids at the binding site, and the reconstitution of hydration gives rise to the anesthetic effect. The reconstitution of hydration water occurs via bipolar interactions. In this study, we observed that the water molecules of interface hydration were released during sevoflurane binding. GA dissolution in the interface water of the binding site was found to result in hydration rearrangements of both the binding site and GA molecule. Computer experiments on the xenon-binding reaction of lysozyme have confirmed that hydrophobic dehydration occurs at the binding site [18]. In this study, water molecule release from sevoflurane binding can be classified as hydrophobic dehydration.

### Contribution of Anesthesia Theoretical Concepts to Clinical Practice

In this study, a common GA binding site in the intersubunit of the target channel GABA<sub>A</sub>R under general anesthesia was revealed, which allowed the binding of various GA structures. Furthermore, the interfacial water at the binding site was demonstrated to be involved in binding. Because the binding sites are common, they are not considered to strictly distinguish GA species. Combined GAs are considered to act in the same way at the binding site, thus acting additively through the site. In anesthesia practice, combined GAs have been used to control loss of consciousness, quality of emergence, and analgesia by drug interactions. This study provides a rationale for the combined use of GA in clinical



practice. The findings of this study may provide insights into the scientific bases for clinical anesthesia and pharmacology.

### Effects of Membrane

The dimer model used for hydration analysis was extracted from the structure of the GABA<sub>A</sub>R-Mb38 mega-body complex (PDB ID: [6i53](#)) in POPC nanodisks and reflects the structure of the membrane protein. However, to focus on the distribution of hydration water molecules in the TMD region, we removed the ECD region and lipids to create a dimer model. Our dimer model does not include lipids and is not suitable for discussing the effects of lipids on intersubunit hydration. In general, many studies have reported functional modifications of ion channels through lipid-protein interactions. GABA<sub>A</sub>R have been reported to have different functions, depending on the components of the reconstituted membrane. We can conceive that the interfacial water of the GA binding site connects to that of the protein surface, lipid interface, and further to that of the channel gate. Fluctuation of the hydration water molecules of the channel gate is involved in hydrophobic gating. The GABA<sub>A</sub>R structure and its hydration water distribution are affected by lipid composition, and the effect is presumed to extend to GA binding and channel function.

### Conclusion

GA binding to GABA<sub>A</sub>R takes place simply by the substitution of hydration water molecules at the binding site and also corresponds to its dispersion and hydration into the interfacial water of the binding site. In this study, we regarded the GA binding process as dissolution in the interfacial water of the GABA<sub>A</sub>R inter-subunit. The GA binding free energy of GABA<sub>A</sub>R correlated with the hydration number of the intersubunit GA binding site and the dehydration number of the GA binding process. The binding selectivity of the intersubunit with weak structural discrimination was due to binding site hydration and GA hydration. The molecular recognition of GA binding via hydration with soft discrimination is understood as the dissolution of interfacial water at the binding site. This molecular recognition mediated by hydration is considered to be involved in the modification of channel open-close dynamics and the mechanism of anesthetic pharmacology, and provides a molecular basis for the legitimacy of the concomitant use of anesthetics in clinical practice.

### Conflict of Interest

The author has no conflict of interest to declare.

### Author Contributions

The author (1) made the study design, computations, and the data analysis or interpretation; (2) drafted and revised the manuscript for all the content; (3) approved the final version of the manuscript to be published; and (4) provides to be accountable for all aspects of the work.

### Data Availability

The computation results of MOE and laboratory notes during the current study are available from the corresponding author on reasonable request.

### Acknowledgements

The authors thank the Department of Anesthesiology and the Central Research Laboratory of Shiga University of Medical Science, as well as the Seto Anesthesia Office for writing and Editage for English language editing.

### References

- [1] Woodbridge, P. D. Changing concepts concerning depth of anesthesia. *Anesthesiology* 18, 536-550 (1957). <https://doi.org/10.1097/0000542-195707000-00002>
- [2] Rengel, K. F., Pandharipande, P. P., Hughes, C. G. Postoperative delirium. *Presse Med* 47, e53-e64 (2018). <https://doi.org/10.1016/j.lpm.2018.03.012>
- [3] Sprung, J., Roberts, R. O., Knopman, D. S., Olive, D. M., Gappa, J. L., Sifuentes, V. L., et al. Association of mild cognitive impairment with exposure to general anesthesia for surgical and nonsurgical procedures: A population-based study. *Mayo Clin. Proc.* 91, 208-217 (2016). <https://doi.org/10.1016/j.mayocp.2015.10.023>

- [4] Belrose, J. C., Noppens, R. R. Anesthesiology and cognitive impairment: A narrative review of current clinical literature. *BMC Anesthesiol.* 19, 241 (2019). <https://doi.org/10.1186/s12871-019-0903-7>
- [5] Franks, N. P. Molecular targets underlying general anaesthesia. *Br. J. Pharmacol.* 147 Suppl 1, S72-S81 (2006). <https://doi.org/10.1038/sj.bjp.0706441>
- [6] Brown, E. N., Pavone, K. J., Naranjo, M. Multimodal general anesthesia: Theory and practice. *Anesth. Analg.* 127, 1246-1258 (2018). <https://doi.org/10.1213/ANE.0000000000003668>
- [7] Olsen, R. W., Sieghart, W. GABA<sub>A</sub> receptors: Subtypes provide diversity of function and pharmacology. *Neuropharmacology* 56, 141-148 (2009). <https://doi.org/10.1016/j.neuropharm.2008.07.045>
- [8] Laverty, D., Desai, R., Uchanski, T., Masiulis, S., Stec, W. J., Malinauskas, T., et al. Cryo-EM structure of the human  $\alpha_1\beta_3\gamma_2$  GABA<sub>A</sub> receptor in a lipid bilayer. *Nature* 565, 516-520 (2019). <https://doi.org/10.1038/s41586-018-0833-4>
- [9] Jayakar, S. S., Zhou, X., Chiara, D. C., Jarava-Barrera, C., Savechenkov, P. Y., Bruzik, K. S., et al. Identifying drugs that bind selectively to intersubunit general anesthetic sites in the  $\alpha_1\beta_3\gamma_2$  GABA<sub>A</sub>R transmembrane domain. *Mol. Pharmacol.* 95, 615-628 (2019). <https://doi.org/10.1124/mol.118.114975>
- [10] Woll, K. A., Zhou, X., Bhanu, N. V., Garcia, B. A., Covarrubias, M., Miller, K. W., et al. Identification of binding sites contributing to volatile anesthetic effects on GABA type A receptors. *FASEB J.* 32, 4172-4189 (2018). <https://doi.org/10.1096/fj.201701347R>
- [11] Nourmahnad, A., Stern, A. T., Hotta, M., Stewart, D. S., Ziemba, A. M., Szabo, A., et al. Tryptophan and cysteine mutations in M<sub>1</sub> helices of  $\alpha_1\beta_3\gamma_{2L}$  g-aminobutyric acid type A receptors indicate distinct intersubunit sites for four intravenous anesthetics and one orphan site. *Anesthesiology* 125, 1144-1158 (2016). <https://doi.org/10.1097/ALN.0000000000001390>
- [12] Maldifassi, M. C., Baur, R., Sigel, E. Functional sites involved in modulation of the GABA<sub>A</sub> receptor channel by the intravenous anesthetics propofol, etomidate and pentobarbital. *Neuropharmacology* 105, 207-214 (2016). <https://doi.org/10.1016/j.neuropharm.2016.01.003>
- [13] Urban, B. W. The site of anesthetic action. in *Handb. Exp. Pharmacol.* (Schüttler, J., Schwilden, H. ed.) vol. 182, pp. 3-29 (Springer, Berlin, 2008). [https://doi.org/10.1007/978-3-540-74806-9\\_1](https://doi.org/10.1007/978-3-540-74806-9_1)
- [14] Meyer, H. Zur theorie der alcohonarkose. *Arch. Exp. Pathol. Pharmacol.* 42, 109-118 (1899). <https://doi.org/10.1007/BF01834479>
- [15] Seto, T., Kato, M., Koyano, K. Molecular discrimination of barbital enantiomer at the propofol binding site of the human  $\beta_3$  homomeric GABA<sub>A</sub> receptor. *CBIJ* 18, 154-163 (2018). <https://doi.org/10.1273/cbij.18.154>
- [16] Franks, N. P., Lieb, W. R. Mapping of general anaesthetic target sites provides a molecular basis for cutoff effects. *Nature* 316, 349-351 (1985). <https://doi.org/10.1038/316349a0>
- [17] Johnson, F. H., Flagler, E. A. Hydrostatic pressure reversal of narcosis in tadpoles. *Science* 112, 91-92 (1950). <https://doi.org/10.1126/science.112.2899.91.b>
- [18] Imai, T., Isogai, H., Seto, T., Kovalenko, A., Hirata, F. Theoretical study of volume changes accompanying xenon-lysozyme binding: Implications for the molecular mechanism of pressure reversal of anesthesia. *J. Phys. Chem. B* 110, 12149-12154 (2006). <https://doi.org/10.1021/jp056346j>
- [19] Goto, J., Kataoka, R., Muta, H., Hirayama, N. ASEDock-docking based on alpha spheres and excluded volumes. *J. Chem. Inf. Model.* 48, 583-590 (2008). <https://doi.org/10.1021/ci700352q>
- [20] Seto, T., Isogai, H., Ozaki, M., Nosaka, S. Noble gas binding to human serum albumin using docking simulation: Nonimmobilizers and anesthetics bind to different sites. *Anesth. Analg.* 107, 1223-1228 (2008). <https://doi.org/10.1213/ane.0b013e31817f1317>
- [21] Kovalenko, A., Hirata, F. Three-dimensional density profiles of water in contact with a solute of arbitrary shape: A RISM approach. *Chem. Phys. Lett.* 290, 237-244 (1998). [https://doi.org/10.1016/S0009-2614\(98\)00471-0](https://doi.org/10.1016/S0009-2614(98)00471-0)
- [22] Beglov, D., Roux, B. An integral equation to describe the solvation of polar molecules in liquid water. *J. Phys. Chem. B* 101, 7821-7826 (1997). <https://doi.org/10.1021/jp971083h>
- [23] Imai, T., Hiraoka, R., Kovalenko, A., Hirata, F. Water molecules in a protein cavity detected by a statistical-mechanical theory. *J. Am. Chem. Soc.* 127, 15334-15335 (2005). <https://doi.org/10.1021/ja054434b>
- [24] Hikiri, S., Hayashi, T., Inoue, M., Ekimoto, T., Ikeguchi, M., Kinoshita, M. An accurate and rapid method for calculating hydration free energies of a variety of solutes including proteins. *J. Chem. Phys.* 150, 175101 (2019). <https://doi.org/10.1063/1.5093110>

- [25] Labute, P. Protonate3D: Assignment of ionization states and hydrogen coordinates to macromolecular structures. *Proteins* 75, 187-205 (2009). <https://doi.org/10.1002/prot.22234>
- [26] Molecular Operating Environment (MOE) 2020.09. 2020. Chemical Computing Group ULC. Montreal, Canada.
- [27] Ponder, J. W., Case, D. A. Force fields for protein simulations. *Adv. Protein Chem.* 66, 27-85 (2003). [https://doi.org/10.1016/s0065-3233\(03\)66002-x](https://doi.org/10.1016/s0065-3233(03)66002-x)
- [28] Gerber, P. R., Muller, K. MAB, a generally applicable molecular force field for structure modelling in medicinal chemistry. *J. Comput. Aided Mol. Des.* 9, 251-268 (1995). <https://doi.org/10.1007/BF00124456>
- [29] Labute, P. The generalized Born/volume integral implicit solvent model: Estimation of the free energy of hydration using London dispersion instead of atomic surface area. *J. Comput. Chem.* 29, 1693-1698 (2008). <https://doi.org/10.1002/jcc.20933>
- [30] db\_Dockscore 2016.01.07, 2016. MOLSIS Inc. Tokyo, Japan.
- [31] Corbeil, C. R., Williams, C. I., Labute, P. Variability in docking success rates due to dataset preparation. *J. Comput. Aided Mol. Des.* 26, 775-786 (2012). <https://doi.org/10.1007/s10822-012-9570-1>
- [32] Clark, A. M., Labute, P. 2D depiction of protein-ligand complexes. *J. Chem. Inf. Model.* 47, 1933-1944 (2007). <https://doi.org/10.1021/ci7001473>
- [33] Pierotti, R. A. The solubility of gases in liquids. *J. Phys. Chem.* 67, 1840-1845 (1963). <https://doi.org/10.1021/j100803a024>
- [34] Pierotti, R. A. Aqueous solutions of nonpolar gases. *J. Phys. Chem.* 69, 281-288 (1965). <https://doi.org/10.1021/j100885a043>
- [35] King, E., Aitchison, E., Li, H., Luo, R. Recent developments in free energy calculations for drug discovery. *Front. Mol. Biosci.* 8, 712085 (2021). <https://doi.org/10.3389/fmolb.2021.712085>
- [36] Koelblinger, P., Thuerigen, O., Dummer, R. Development of encorafenib for BRAF-mutated advanced melanoma. *Curr. Opin. Oncol.* 30, 125-133 (2018). <https://doi.org/10.1097/CCO.0000000000000426>
- [37] Sebel, L. E., Richardson, J. E., Singh, S. P., Bell, S. V., Jenkins, A. Additive effects of sevoflurane and propofol on gamma-aminobutyric acid receptor function. *Anesthesiology* 104, 1176-1183 (2006). <https://doi.org/10.1097/00000542-200606000-00012>
- [38] Alkire, M. T., Hudetz, A. G., Tononi, G. Consciousness and anesthesia. *Science* 322, 876-880 (2008). <https://doi.org/10.1126/science.1149213>
- [39] Nakasako, M. Water-protein interactions from high-resolution protein crystallography. *Philos. Trans. R. Soc. Lond. B Biol. Sci.* 359, 1191-1206 (2004). <https://doi.org/10.1098/rstb.2004.1498>
- [40] Aryal, P., Sansom, M. S., Tucker, S. J. Hydrophobic gating in ion channels. *J. Mol. Biol.* 427, 121-130 (2015). <https://doi.org/10.1016/j.jmb.2014.07.030>
- [41] Rao, S., Klesse, G., Lynch, C. I., Tucker, S. J., Sansom, M. S. P. Molecular simulations of hydrophobic gating of pentameric ligand gated ion channels: Insights into water and Ions. *J. Phys. Chem. B* 125, 981-994 (2021). <https://doi.org/10.1021/acs.jpcc.0c09285>
- [42] Ueda, I., Mashimo, T. Anesthetics expand partial molal volume of lipid-free protein dissolved in water: Electrostriction hypothesis. *Physiol. Chem. Phys.* 14, 157-164 (1982).

